FORTH-ICS / TR-343 September 2004

SIMUUN: A Simulation Environment for Undulatory Locomotion†

M. Sfakiotakis and D.P. Tsakiris

Abstract

This report presents SIMUUN, a block-based simulation environment, which has been developed on top of Matlab/Simulink^{TM}, in order to facilitate research into various aspects of undulatory locomotion in biology and robotics, including assessing the effect of different body configurations on gait generation. Simulations of snake-like mechanisms are set up in this environment by connecting customisable SIMUUN body segment modules via appropriate joint blocks, which are activated either by explicit or by neuromuscular joint control modules, to propagate a travelling wave along the mechanism. Several force models are included in SIMUUN to characterise the interaction with the locomotion environment, and emulate crawling, walking and swimming. The simulation tools developed were used to study anguilliform swimming in robotics and in biology. Related simulation results are presented to illustrate the versatility of these tools and the potential of their use in a variety of domains.

Keywords: Biomechanical modelling, undulatory locomotion, robotics, biology, Anguilla anguilla eel.

† This work was partially supported by the EU IST-2001-34181 project BIOLOCH.

SIMUUN:
A Simulation Environment for Undulatory Locomotion

M. Sfakiotakis and D.P. Tsakiris

Computational Vision and Robotics Laboratory
Institute of Computer Science (ICS)
Foundation for Research and Technology — Hellas (FORTH)
Science and Technology Park, Heraklio, Crete
P.O. Box 1385, GR-711-10 Greece

Web: http://www.ics.forth.gr/cvrl
E-mail: {sfakios | tsakiris}@ics.forth.gr
Tel: +30 2810 391708, Fax: +30 2810 391601

Technical Report FORTH-ICS / TR-343 — September 2004

©Copyright 2004 by FORTH

Abstract

This report presents SIMUUN, a block-based simulation environment, which has been developed on top of Matlab/Simulink^{TM}, in order to facilitate research into various aspects of undulatory locomotion in biology and robotics, including assessing the effect of different body configurations on gait generation. Simulations of snake-like mechanisms are set up in this environment by connecting customisable SIMUUN body segment modules via appropriate joint blocks, which are activated either by explicit or by neuromuscular joint control modules, to propagate a travelling wave along the mechanism. Several force models are included in SIMUUN to characterise the interaction with the locomotion environment, and emulate crawling, walking and swimming. The simulation tools developed were used to study anguilliform swimming in robotics and in biology. Related simulation results are presented to illustrate the versatility of these tools and the potential of their use in a variety of domains.

Keywords: Biomechanical modelling, undulatory locomotion, robotics, biology, Anguilla anguilla eel.

1. Introduction

The development of undulatory robotic locomotors, namely serially connected, multilink articulated robots, propelling themselves by body shape undulations, has attracted significant interest in view of emerging applications related to site inspection, search-and-rescue missions, mine clearance, and even endoscopy or planetary exploration. Advantages associated with

undulatory robots include terrain adaptability, modularity and redundancy, as well as their potential for use as combined locomotors and end-effectors. Although most of the existing such robots utilize passive wheels to realize serpentine locomotion (see [1], [2], [3] and references therein), prototypes which crawl on their underside, and do not rely on wheels (e.g. [4], [5], and [6]), as well as undulatory swimming robots (e.g. [7] and [8]) have also been developed. Inspiration is provided by biological organisms, since locomotion by transversal whole-body waves is widespread among elongated, narrow animals. It is primarily an aquatic trait (termed *anguilliform* swimming), employed by animals ranging in size from larvae and marine annelids to sea snakes and eels, but is also utilized in a terrestrial environment by snakes and lizards, while also being common among amphibians (e.g. salamanders and axolotls).

An undulating body (biological or robotic) can achieve locomotion through appropriate coupling of internal shape changes (typically a wave travelling along the body) to external motion constrains (typically frictional forces arising from the interaction with the locomotion environment). The effect of both these aspects needs to be considered when analysing undulatory locomotion, in order to, for example, design efficient such robotic prototypes. The large number of parameters involved in this process (e.g. number and size of body links, travelling wave properties, characteristics of the interaction with the environment, etc.) is increased even further when more complex architectures (e.g. parapodial appendages, neuromorphic control schemes, sensor-based reactive behaviours, etc.) are considered, thus highlighting the need for powerful and versatile software design tools. In this context, SIMUUN, a simulation environment based on Matlab/Simulink™ [9], has been developed, in order to facilitate research into various aspects of undulatory robotic locomotion, which include assessing the effect of different body configurations, modelling the interaction with the environment, and applying neuromorphic control schemes. At the core of this development is the SimMechanics physical modelling toolbox of Simulink, used to create libraries containing integrated "body segment" modules, which are serially connected to simulate the mechanics of planar articulated robots. The developed set of tools has already facilitated the design, simulation and analysis of the polychaete-like undulatory robotic prototype presented in [6]. Since SIMUUN is versatile, expandable and relatively straightforward to work with, it can have additional uses in computational neuroethology [10], or as a predictive tool in biological studies of undulatory locomotion [11].

Section 2 of the report introduces the main components of SIMUUN. Sections 3 and 4 detail their use, in the context of undulatory swimming, and present issues, related to body wave generation, force modelling, and performance analysis. Additional example applications are then provided, involving the use of SIMUUN to develop a sensor-based undulatory centering behaviour (section 5) and to replicate biological data on eel swimming (section 6). This last application demonstrates the potential of SIMUUN as a tool for data analysis and experiment design in biological studies.

2. The Simulation Environment

SIMUUN has been created on top of the Simulink substrate, to take advantage of its modular, block-based architecture and of the numerous related software tools, for building and integrat-

ing the main components involved in simulating an undulatory locomotor. These components (shown in Fig. 1a) are: (i) the body mechanical model, (ii) the body shape control model, and (iii) the force model of the body's interaction with the environment. A distance sensing module, coupled to a model of the locomotion environment layout, have also been created, to facilitate the study of sensor-based, closed-loop control schemes.

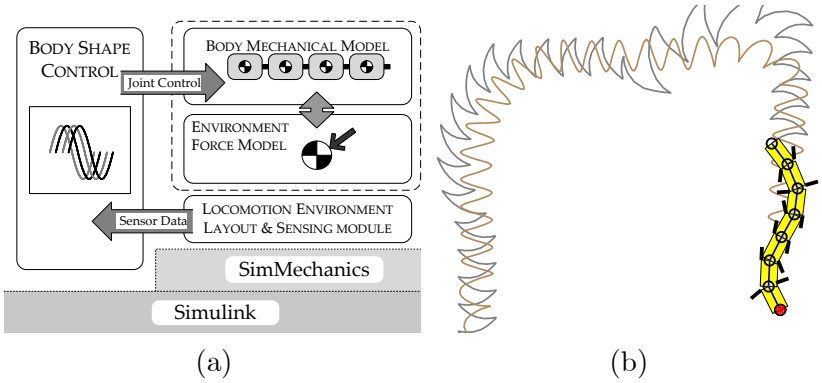

Figure 1: (a) Main components of the simulation environment. (b) Still frame from an animation, created with the results of a simulation of polychaete annelid locomotion.

Development is within Simulink's graphical interface, using simple and intuitive manipulations of the undulatory component modules to construct the desired configurations. Setting up a basic simulation of an undulatory mechanism within SIMUUN involves the following steps: The mechanical model of the body is initially created, by serially connecting "body segment modules", using simple drag-and-drop operations. In a similar fashion, the appropriate "body shape control module" is inserted in the model and linked to the mechanical model subsystem, to provide the joint actuation signals for the undulatory mechanism. The environment force model to be used, along with miscellaneous other parameters of the simulation (e.g. its time range), are set in a Matlab script file. For simulations involving sensor-based control schemes, additional "sensing blocks", coupled to Matlab script files describing the layout of 2D wall-like features in the locomotion environment, may be incorporated in the Simulink model. During the simulation, a number of variables (link positions, joint velocities, applied forces etc.) is being recorded, to allow the user a thorough analysis of the results. A number of peripheral Matlab scripts facilitate tasks such as batch-run simulations and animation of results (an example is shown in Fig. 1b). By default, the `ode45` variable step continuous solver is employed to carry out the numerical integration of the deployed models, although any of the available Simulink solvers [9] can be used, if required.

The SIMUUN library blocks have been created using standard Simulink/SimMechanics blocks and, although they are generic enough, even their internal structure can be easily modified by the user, and tailored to the requirements of particular applications, should such a need arise. Furthermore, all the available Matlab/Simulink add-ons (toolboxes, coding options, etc.) can be used within this framework to implement additional features. Simulation runs with multiple undulatory mechanisms, e.g. for developing cooperative behaviours, are also readily supported in SIMUUN.

2.1 Mechanical Modelling of the Body

The body mechanics are modelled using the SimMechanics toolbox in Simulink. SimMechanics simulates rigid body motions, forces and torques, employing the available numerical solvers to integrate the equations of motion. These are automatically formed by SimMechanics, after the user has set up the block diagram of the simulated mechanism, without requiring an analytical model of the system. In order to simulate multi-segment undulatory mechanisms, a "body segments library" (BSL, for short) has been developed, which contains integrated 2D segment modules, with individual settings for their mass, shape (cylindrical or rectangular) and dimensions. The library is shown in Fig. 2, while the internal structure of the body segments is illustrated in Fig. 3. Each BSL module incorporates the main body link (block **a** in Fig. 3) with a planar revolute joint (Fig. 3-**b**), through which segments are connected together to form serial chains (Fig. 4). Two variants of the body segment modules are provided, differentiated by whether the motion of the revolute joints is provided in terms of prescribed joint angle variations, or by joint torque signals (see section 3.2). In both cases, this is achieved via special "joint actuation" SimMechanics blocks (Fig. 3-**c**), driven by the appropriate shape control module. Of particular interest is the simulation of the locomotion of segmented worms of the polychaete annelid class [6]. For this purpose, additional BSL modules have been created, which are equipped with twin "parapodial" appendages (Fig. 3-**f**, visible in Fig. 1b), placed at opposing sides along the body link, and connected to it via active revolute joints. Special SimMechanics "body sensor" blocks (Fig. 3-**e**), provide direct access to the link positions, velocities and applied forces, and to the joint torques and angles, during the simulation. Apart from data logging, this information is used to implement the distance sensor modules, presented in section 2.4.

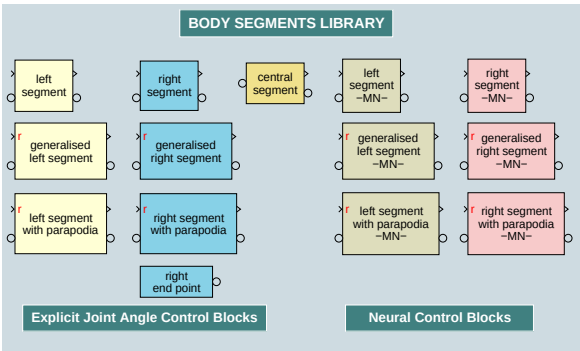

Figure 2: The body segments library (BSL) of the simulation environment.

This modular, library-based scheme allows for different body configurations to be set up easily and with minimal troubleshooting, using simple drag-and-drop operations. Mechanisms containing an arbitrary number of segments, each with different properties (even mixing plain and parapodia-bearing blocks), can be created very quickly, in order to evaluate their performance.

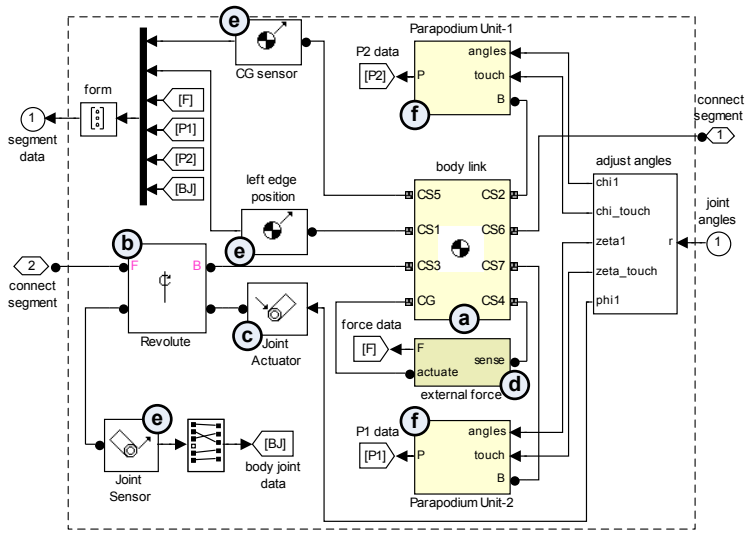

Figure 3: The internal structure of a body segment module with parapodia.

2.2 Modelling the Interaction with the Environment

Locomotion of an undulating body results from the coupling of its internal shape changes to external motion constraints. These constraints are usually due to external (frictional) forces, resisting the motion of the links and applied through the interaction with the locomotion environment. Two different force models, developed to approximate the characteristics of this interaction for both the aquatic and terrestrial locomotion, have been incorporated in SIMUUN. Both models are resistive, i.e. the force on a body segment depends on its velocity (rather than acceleration), and they involve decoupled force components in the normal and tangential direction of motion. A fluid drag model (detailed in section 3.1) is used to emulate swimming, while for crawling a more generic friction model has been developed. The latter combines stiction (static friction), Coulomb and viscous damping, as well as the Stribeck effect [12], and anisotropic characteristics, in an effort to allow coverage of the wider range of tribological phenomena encountered in different terrestrial substrates. The blocks implementing the selected force model are embedded in the structure of the body segment modules (Fig. 3-**d**) and they utilize special "body force" SimMechanics blocks to apply the external forces. The link velocities, necessary for implementing the resistive force models, are obtained directly from the "body sensor" blocks described in the previous section.

2.3 Modelling Body Shape Control

Fundamental to all undulatory locomotion schemes (both biological and robotic) is the propagation of a travelling wave along the locomoting body. In SIMUUN, the "shape control library" (SCL, for short) comprises a number of modules, built with standard Simulink blocks, which implement different methods to generate the travelling wave, by controlling the joints in the body's mechanical model. Two of these methods (explicit joint actuation and neuromuscular actuation) are presented in more detail, within the context of elongated body swimming, in section 3.2. For simulations involving undulatory mechanisms with parapodial appendages,

the respective body shape control modules also provide the control signals for the parapodial joints. The SCL modules are also used for implementing sensor-based, closed-loop controllers, as it is demonstrated in section 5.

2.4 Locomotion Environment Model and Sensing Module

The current version of SIMUUN includes modules which emulate distance sensing elements, and implement simple 2D models of the world that the mechanism is presumed to be operating in, typically a maze-like environment. The latter is defined in terms of (consecutive) line segments, by providing their 2D position coordinates in a Matlab script file. The sensor modules then operate by calculating the distance of the geometric centers of all the mechanism's link (whose coordinates are readily available from the "body sensor" SimMechanics blocks) from these line segments. The developed modules assume pairs of distance sensors, mounted on each link center, and aiming at user-defined symmetric angles with respect to the main axis of the link. Each link may be endowed with more than one sensor pairs, to realize the full sensing array considered for different configurations of the undulatory mechanism (an example is shown in Fig. 13). Variations of the sensing subsystem to consider the effect of noise in the distance measurements, or to implement simpler whisker-like sensing elements have also been developed. An example application utilizing the sensing blocks is described in section 5. Additional sensory modalities and locomotion environments are easy to incirporate in SIMUUN, based on the flexibility of Matlab/Simulink, and will be included in future versions of the simulation environment.

3. Setting up Simulations of Elongated-Body Swimming

By appropriate choice of the various options available for the simulator components (e.g. number and dimensions of body segments, travelling wave formulation, and force model used), different configurations for the undulatory mechanism, relating to a varying degree to biological analogues, can be studied. A primary motivation behind such efforts is the abstraction of biological locomotion features, in order to apply them to robotic designs [6]. Alternatively, models which incorporate detailed shape and kinematic data of animals, could be used as predictive tools for understanding their control and dynamics. An example of such an application is provided here, with SIMUUN being used to set up simulations capturing the key aspects of anguilliform swimming. The analysis, which also highlights details and usage of the various components of the simulation environment, is based on a basic undulatory mechanism, built using BSL modules (Fig. 4), and comprising $N = 7$ identical links, each with a mass m uniformly distributed across its length l.

3.1 Fluid Drag Model

Details of the fluid drag model, which is integrated in the body segment modules of SIMUUN, and is used to simulate the interaction of undulatory mechanisms with the aquatic environ-

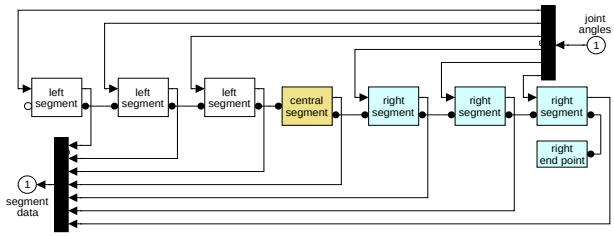

Figure 4: Mechanical model of the undulatory mechanism, constructed by serially connecting seven body segment modules.

ment, are provided here. The model is a first approximation of the hydrodynamics invloved, under the following assumptions: (i) the Reynolds number is high enough for inertial forces to dominate over viscous effects (roughly for $400 < Re < 4 \cdot 10^5$), (ii) the fluid is stationary, so that the force of the fluid on a single link is due only to the motion of that link, and (iii) the pressure differentials (responsible for generating the drag forces resisting the link's motion) are considered independently for the tangential and normal directions. Then, the two components of the force applied to the ith link are respectively obtained as:

$$\begin{aligned} F_T^i &= -\lambda_T \operatorname{sgn}(v_T^i) \cdot (v_T^i)^2 \\ \text{and} \quad F_N^i &= -\lambda_N \operatorname{sgn}(v_N^i) \cdot (v_N^i)^2 \end{aligned} \tag{1}$$

where v_T^i and v_N^i are the tangential and normal components of the velocity of the ith link. The drag coefficients associated with each force component are denoted as λ_T and λ_N. Their value can be estimated as:

$$\lambda = \frac{1}{2}\rho C S \tag{2}$$

where S is the effective area of the link, ρ is the fluid density and C is a shape coefficient. The notion of decoupled forces in the normal and tangential direction of link motion can be traced to Taylor's resistive analysis of elongated animal swimming [13], and is considerably simpler to calculate and integrate with the body dynamics than any model which requires solving the Navier-Stokes equations. It has therefore been used quite extensively in the literature (e.g. [8], [14] and [10]), despite ignoring secondary effects of water movement. Since the assumptions of this model restrict its scope to the inviscous swimming of elongated animals, it cannot be applied to the undulatory swimming of microorganisms (e.g. nematodes and flagella), nor to the more sophisticated swimming modes encountered in fish [15].

The ratio λ_N/λ_T of the drag coefficients in (1) is a key parameter in undulatory locomotion. The elongated body of anguilliform swimming animals (e.g. eels) is smooth and of elliptical cross-section, so that $\lambda_T << \lambda_N$ (Lighthill [16] estimates $\lambda_N/\lambda_T \simeq 10$ for a swimming grass-snake). The overall locomotion direction is then opposite to that of the wave direction, and therefore, forward propulsion is achieved by body waves propagating from head to tail; moreover, smooth elongated animals can swim backwards by reversing the propulsive wave [17]. If the animal body is not smooth, the propulsive component of the tangential force may be greater than that of the normal force (corresponding to $\lambda_N/\lambda_T < 1$), and locomotion is along

the direction of wave propagation. Forward motion would then be achieved by a tail-to-head wave. This is indeed the case for the locomotion of polychaete, whose body affords a significant amount of roughness, mainly due to the laterally projecting appendages (parapodia) distributed along their body [18]. Henceforth, we will use the terms *smooth-body configuration* and *rough-body configuration*, to distinguish between these two modes of undulatory locomotion.

3.2 Shape Control of the Body

Two methods for generating a travelling body wave to obtain undulatory locomotion in the simulated mechanical models are presented in this section. The first method is based on the assumption of direct control of the mechanism's joint angles, while the second one is a neural control scheme, where the control inputs are the joint torques. Both approaches have been implemented as SCL modules in SIMUUN, and can be used in closed-loop configurations.

3.2.1 Explicit Joint Angle Control

The most straightforward way to explicitly generate a travelling wave in a serial chain of N links is by having the joint angles vary sinusoidally, with a common frequency f and a constant phase lag ϕ_{lag} between consecutive joints:

$$\phi_i(t) = A_i \sin(2\pi f t + i\phi_{lag}) - \psi, \qquad i = 1, ..., (N-1) \tag{3}$$

where A_i is the maximum angular deflection for the ith joint (usually $A_i = A$ is assumed). The angular offset ψ provides a means for steering along curved paths, and is set to $\psi = 0$ for locomotion in a straight line. The propagation direction for the wave depends on the sign of the phase lag parameter, and is from link-N to link-1 for $\phi_{lag} > 0$. The condition $\phi_{lag} = \pm 2\pi/N$ yields (exactly) one wavelength of the propulsive wave across the undulating body, with beneficial effects on the propulsive efficiency. For links of identical length, the formulation of (3) produces a sinusoidal body shape, which is shown in Fig. 5 for the seven-link mechanism. The propagation velocity of the wave is calculated as $V = fw$, where w is the resulting wavelength.

Closed-loop control schemes utilising (3) may also be set up, whereby the parameters A and f are used to alter the speed of locomotion, while changes in ψ impose orientation changes. Appropriate such SCL modules have been created, which receive input by "controller" blocks, typically developed by the user for implementing e.g. sensor-based reactive behaviours.

3.2.2 Neural Control

A biologically-motivated body shape control method is based on central pattern generators (CPGs), which are neuronal circuits able to produce rhythmic motor patterns in an organism (for swimming, flying, breathing, etc.), even in the absence of sensory input or input from higher cognitive elements. Their behaviour depends both on the intrinsic properties of the neurons that form the network, as well as on the properties of the synapses among them (connectivity, strength, etc.). Inspired by models of the CPG which controls the undulatory

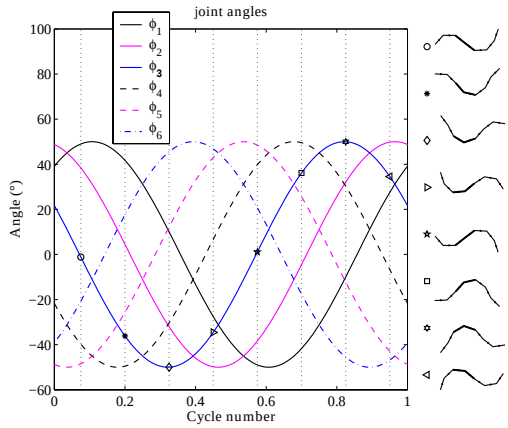

Figure 5: Relation between the joint angles and the overall body, for $N = 7$, $\phi_{lag} = 2\pi/N$, and $A = 50°$. The markers follow the variation of ϕ_3, the joint angle between links 3 and 4 (shown bold on the right).

swimming of the lamprey (e.g. [14], [10]), SCL modules realizing neuromuscular body shape control were developed. They are based on a connectionist CPG circuit, which is modelled as a chain of (identical) segmental oscillators, properly interconnected to generate a wave of joint activation. Each segmental oscillator is formed by two symmetrical sub-networks, which create oscillations through mutual inhibition. They comprise interneurons and motoneurons, which are all modelled as leaky integrators. The torque eventually applied to each of the body joints is determined by the outputs of the corresponding motoneurons, activating a pair of antagonistic lateral muscles, which are simulated using a spring-and-damper muscle model (Fig. 6). The characteristics of the motoneuron outputs can be altered by tonic (i.e. non-oscillating) inputs to the left and right sub-networks of the segmental oscillators [6].

The modules developed for neuronal control in SIMUUN comprise blocks which implement the basic segmental oscillator units. These are then serially connected by the user to form the desired CPG circuit, as illustrated in Fig. 7. Both the interneuronal and the intersegmental connectivities of the CPG are defined using Matlab scripts, to facilitate the investigation of different architectures, e.g. by using optimisation schemes based on genetic algorithms.

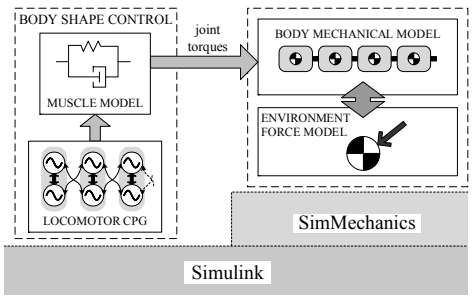

Figure 6: Neural control-based simulation scheme.

For our simulations with the basic seven-link mechanism, a body CPG comprising 20 segmental oscillators, was constructed. The motoneuron outputs from (roughly) every third

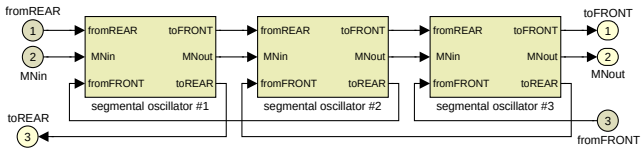

Figure 7: CPG circuit construction within SIMUUN.

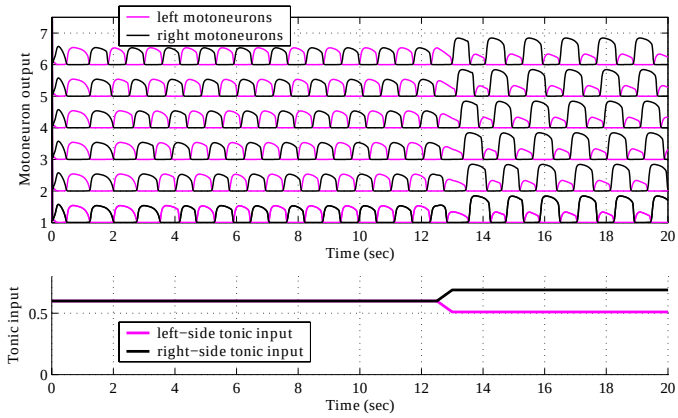

Figure 8: Tonic input and resulting motoneuron outputs of the CPG segmental oscillators, controlling the body joints.

oscillator were utilized to provide torque signals to the six body joints, through the antagonistic muscles. Motion in a straight line is obtained by symmetric activation of the two sides of the body CPG, via equal tonic inputs, while turning motions are instigated by unequal tonic input to them (Fig. 8). Rapid transition in the motoneuron outputs, when varying the tonic input, is a key feature for smooth steering of the mechanism, and was found to be closely related to the type of intersegmental coupling used in the CPG structure. The scheme was successfully applied to both smooth- and rough-body configurations. Since the CPG-based approach provides torque signals to the joints, their exact angular motion depends on the mechanical properties of the segments, as well as on the parameters of the force model used. The resulting joint angles are therefore quite different from the explicitly defined ones (cf. Figs. 9 and 5). This fact, along with the non-straightforward interaction between the tonic input level and the properties of the motoneuron outputs (i.e. frequency and amplitude), renders the precise tuning of the travelling wave parameters difficult, and highlights the benefits of using SIMUUN for design purposes.

In the neural control SCL modules, the tonic input signals are provided by external Simulink blocks, which, for open-loop configurations, are straightforward functions of time (as in Fig. 8). Alternatively, when implementing closed-loop schemes, the tonic input signals are provided by custom "controller" blocks developed by the user (one such example application is presented in section 5).

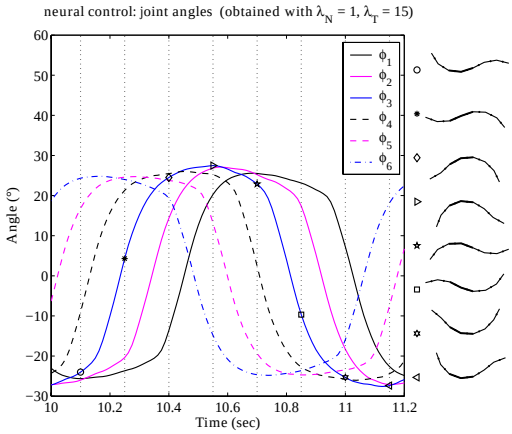

Figure 9: Joint angles and body shape, obtained using neural control to generate the travelling wave.

4. Application: Simulating Qualitative Characteristics of Undulatory Swimming

This section describes the use of SIMUUN to replicate the fundamental characteristics of undulatory swimming, through a series of simulations. In particular, the effect of the joint amplitude A and frequency f of the body travelling wave on swimming velocity and efficiency is assessed for different body configurations, and the main undulatory gaits are produced. The seven-link mechanism is coupled to the explicit body shape control module, which makes use of (3) to generate the propulsive wave, with $\phi_{lag} = 2\pi/N$, $A_i = A$, and $\psi = 0$. Using a simple Matlab script file, the model was run for a range of values for f (up to 4.5 Hz) and A (up to 80°), with simulations performed for both smooth (with $\lambda_T = 1$, $\lambda_N = 10$) and rough (with $\lambda_T = 10$, $\lambda_N = 1$) body configurations. Each time, the mean swimming velocity U was evaluated as the mean rate of displacement for the center of the middle link along the direction of motion, after the initial transient. Positive U values relate to motion in the opposite direction of wave propagation (eel-like locomotion), whilst for negative U values, the body moves in the same direction as the travelling wave (polychaete-like locomotion). The propulsion efficiency $|U/V|$ (see [15], [16]), was also calculated.

The results are compatible with the predictions in [13], and correlate well with biological observations. For both body configurations, the velocity U was found to be linearly dependent on f, which is consistent with data on anguilliform-swimming animals [17], as well as with the predictions of other analytical approaches [8] and simulations [4]. This renders the U/V ratio independent of f. Results are then summarized in Fig. 10. In the smooth body case, U is moderately affected by A, with a distinct maximum appearing for $A \simeq 45°$. In the rough body case, U shows a greater disparity with regard to the undulation amplitude: for values of A below $\sim 40°$ the velocities achieved are very small (particularly compared to the smooth body performance with the same parameters). This is consistent with the slow swimming speed and low efficiency of polychaete locomotion [18], [16]. However, as A is further increased, higher U values are attainable with this type of body configuration (at the expense of significantly increased power requirements).

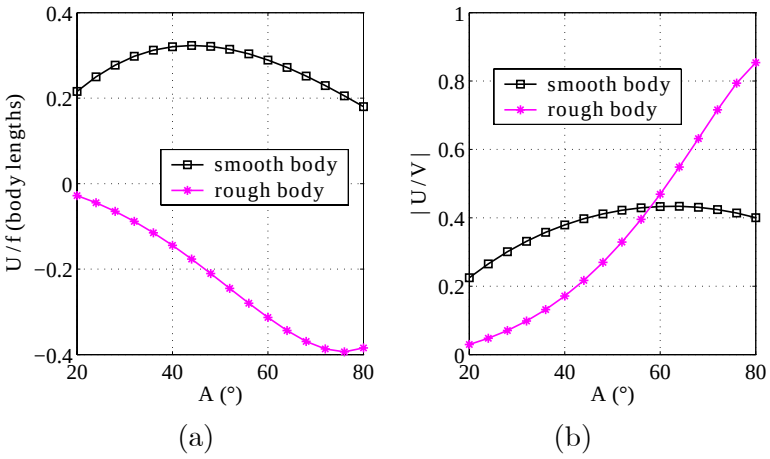

Figure 10: (a) Attained velocity and (b) propeller efficiency for the smooth- and rough-body configurations.

In order to study the effect of the drag coefficients on U, simulations were performed for a range of λ_T and λ_N values, with $f = 1\,\text{Hz}$ for $A = 35°$ and $A = 70°$. Simulations indicated that for both the smooth- and the rough-body configurations, the attained velocity only depends on the ratio of the drag coefficients, rather than on their specific values. Results are summarized in Fig. 11.

Turning motions are obtained by introducing an offset angle $\psi \neq 0$ in the joint oscillations. Simulation results, shown in Fig. 12, indicate that turning is more efficient for the smooth, than for the rough case. During turns in the smooth-body configuration, all links follow the same mean path, while in rough-body locomotion, the mean path of distal links has a distinct offset from the mean path traced by the middle link. Additional locomotion gaits (such as in-place rotation and parallel-parking) have also been implemented using variations of (3) for the evolution of the joint angles ϕ_i. In every case, the direction of motion, both translational and rotational, is determined by the λ_N/λ_T ratio.

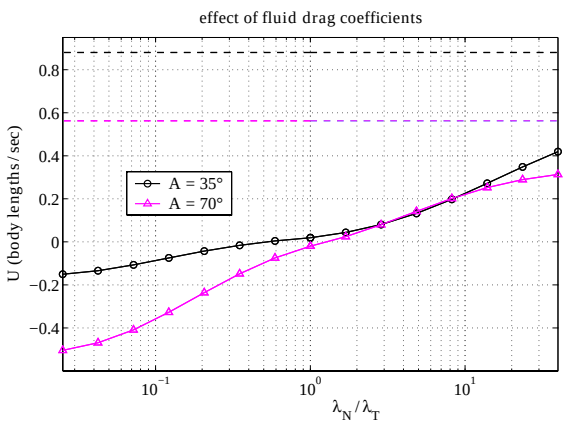

Figure 11: Attained velocities as a function of λ_N/λ_T, for two values of the joint amplitude A. Dashed lines indicate the absolute value of the respective wave velocities V.

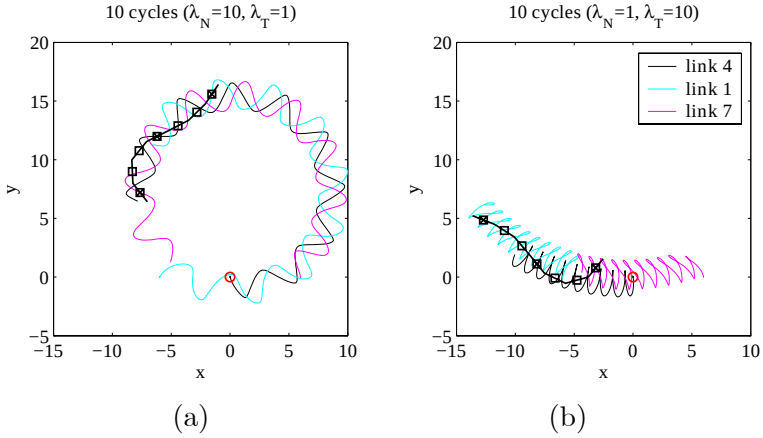

Figure 12: Link trajectories during turning motions, for the smooth- and rough-body configurations, shown in (a) and (b), respectively. Parameters in (3) were set as $A_i = 30°$, $\phi_{lag} = 51.4°$, $\psi = 12°$, and $f = 1$ Hz.

5. Application: Simulating Sensor-Based Neural Control of Undulatory Swimming

This section demonstrates the use of SIMUUN to develop a reactive, sensor-based undulatory behaviour, by implementing a closed-loop setup in the block diagram layout. The specific behaviour presented here is inspired by the centering response exhibited by bees: while flying through narrow gaps, bees tend to fly through the center of the gap, despite their lack of stereoscopic vision and their inability to explicitly estimate distance. The hypothesis put forward is that bees balance the image motion perceived by their two wide field-of-view compound eyes [19]. This bee behaviour inspired the implementation of reactive centering behaviours for nonholonomic mobile robots equipped with laser range finders and panoramic cameras. The corresponding sensor-based control laws employ optical flow information from several distinct "looking" directions in the entire field of view of the panoramic cameras directly in the control loop [20]. Adaptation of such sensor-based control schemes to the significantly more complicated dynamics of undulatory robotic locomotors, using the developed simulation environment is presented next. The central idea is to balance the weighted sum of the distance sensor outputs to the left and right sides of the robot.

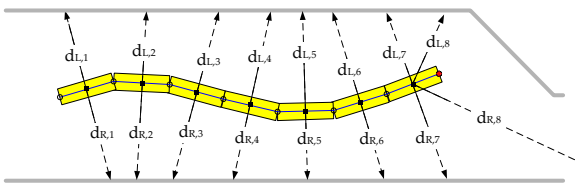

Figure 13: Example configuration of a sensor array for an undulatory mechanism.

For our purposes, the same seven-link undulatory mechanism, coupled to the locomotor CPG described in Section 3.2.2, is considered. Assuming M pairs of distance sensors (see

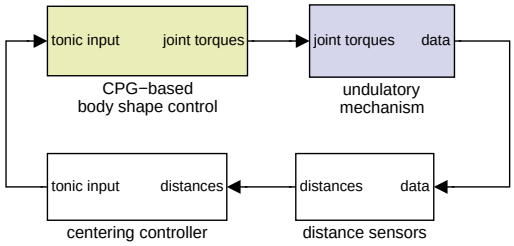

Figure 14: SIMUUN block diagram implementing the undulatory centering behaviour.

section 2.4), and denoting $d_{L,j}$ and $d_{R,j}$ $(1 \leq j \leq M)$ the outputs for such a sensing array (Fig. 13), the generic control law to realize the undulatory centering behaviour is then implemented via the tonic input signals applied to the left and right sides (I_L and I_R, respectively) of the CPG, so that:

$$I_L(t) = 1 - kS(t) \text{ and } I_R(t) = 1 + kS(t), \quad \text{for } k > 0 \tag{4}$$

where the distance metric $S(t)$ is obtained as:

$$S(t) = \frac{1}{\sum_{j=1}^{M} q_j d_{L,j}(t)} - \frac{1}{\sum_{j=1}^{M} q_j d_{R,j}(t)} \tag{5}$$

The weights q_j in (5) determine the relative contribution of the available sensor pairs in calculating $S(t)$.

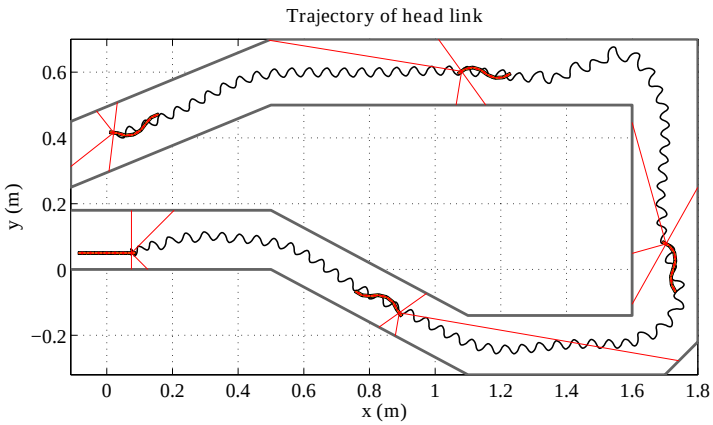

Figure 15: Neural control of the undulatory centering behaviour: trajectory of the head link in the locomotion environment.

This scheme can achieve the undulatory centering behaviour for both smooth- and rough-body configurations. The block diagram developed within SIMUUN to implement the CPG-based undulatory centering behaviour is shown in Fig 14. The sensing array comprised two sensor pairs, mounted on the head link of the mechanism, and aiming at ±45° and ±90° with respect to the link's main axis. The centering controller based on (4) and (5), was implemented

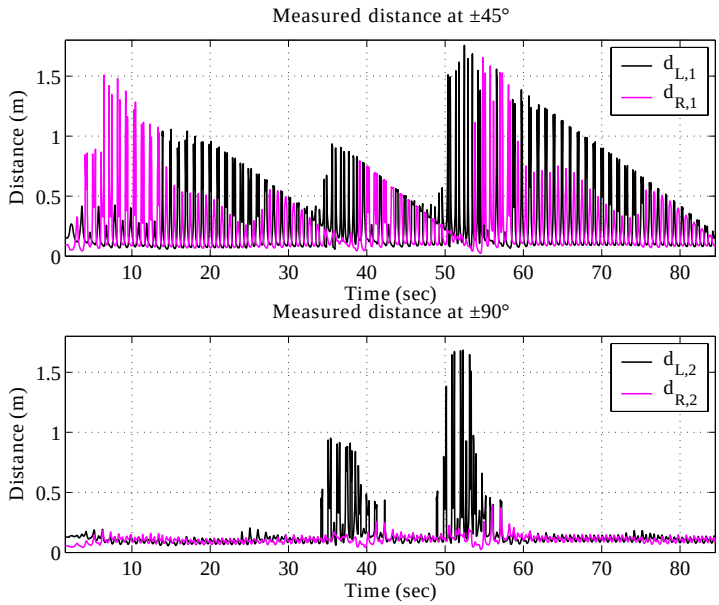

Figure 16: Neural control of the undulatory centering behaviour: outputs of the sensing array utilised.

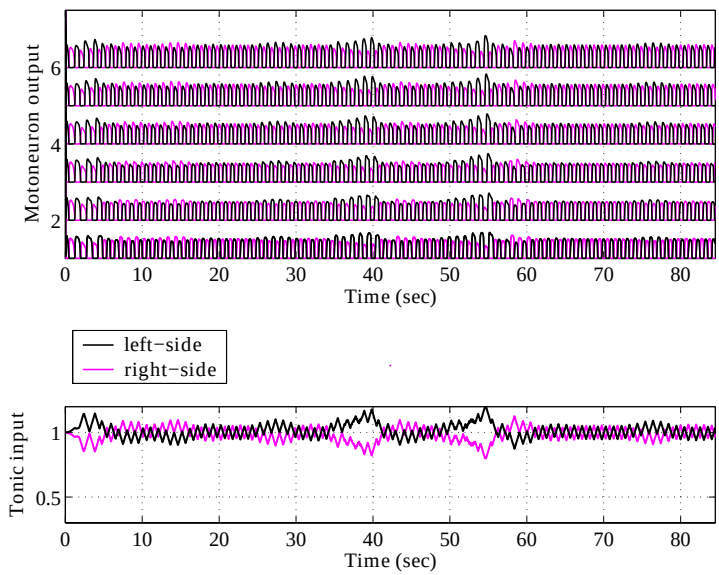

Figure 17: Neural control of the undulatory centering behaviour: Motoneuron outputs (top) and the respective tonic inputs (bottom).

using standard Simulink blocks, with the control law parameters set as $q_1 = q_2 = 1$ and $k = 0.029$. A maze-like environment was then created to test the controller, and simulations were performed using the fluid drag model, assuming a smooth-body configuration for the seven-link mechanism, with $\lambda_N/\lambda_T = 10$. Results, shown in Figs. 15-17, demonstrate the successful application of the sensor-based, neural control scheme to implement this particular undulatory behaviour, the development of which was greatly facilitated by the Simulink framework of SIMUUN.

6. Application: Replicating Biological Data of Undulatory Swimming

This section demonstrates how SIMUUN allows the replication of biological data for organisms locomoting by undulations, thus becoming a useful tool both for the analysis of such data, and for designing new related biological experiments.

Simulations were set up based on the detailed biological data from filmed sequences of swimming of the *Anguilla anguilla* eel, which are provided in [17]. A biomechanical eel model has been constructed, comprising 20 links, of equal length and cylindrical in shape, to reflect the analysis framework in [17], and incorporating the biometric measurements reported therein (total body length $L = 22\,\text{cm}$, and total mass $M = 13\,\text{g}$). The Reynolds number for the reported eel swimming kinematics is around $Re \simeq 3 \cdot 10^4$, thus validating the use of the fluid drag model in the simulations; the drag coefficients were calculated using (2) and set to $\lambda_N = 0.5\,\text{kg/m}$ and $\lambda_T = 0.01\,\text{kg/m}$. The explicit joint angle control scheme is used to generate the travelling wave in the developed eel model.

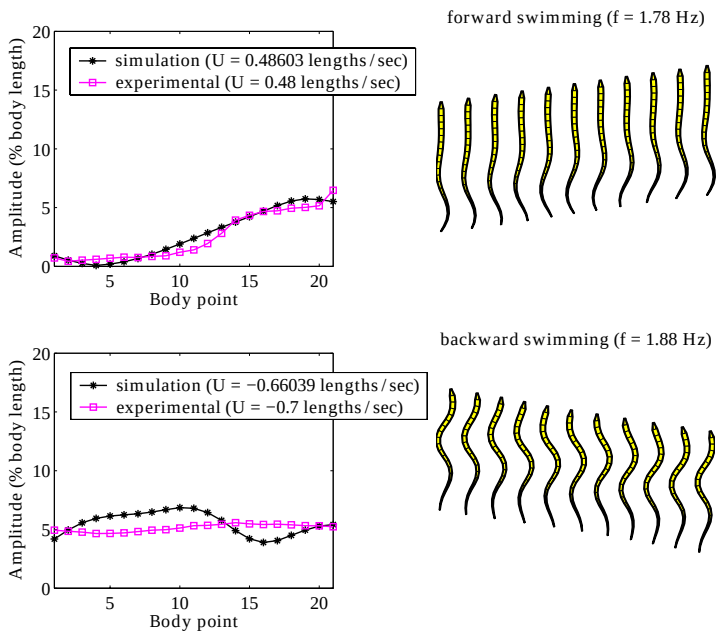

Figure 18: Amplitude profiles (left) and body contour plots (right) for simulations of forward and backward eel swimming. Body points refer to the endpoints of the eel sections considered in [17].

Two simulation runs are presented here, corresponding to two of the representative eel swimming sequences analyzed in [17] (one for forward, and one for backward propulsion). From the pool of biological data for the two selected sequences, the reported frequencies and maximal angles between segments, along with the body contour plots provided, were used to set the parameters f, A_i and ϕ_{lag} in (3). Results were then evaluated by comparing the attained velocities and body amplitude profiles obtained in simulation, against the corresponding measurements in [17]. For both the forward and the backwards sequences, a very good match has been obtained (Fig. 18). A number of additional observations made in [17], on the

eel swimming kinematics and their relation to body shape and mass distribution (regarding, for example, the orientation changes of the head), can also be reproduced with the presented model.

7. Conclusions

The simulation environment presented in this report aims to facilitate the study of undulatory locomotion principles, both in biological organisms and in related robotic implementations. Further extensions to SIMUUN will include the expansion to three-dimensional mechanisms and motions (which is made possible by the built-in support of SimMechanics for 3D models), the incorporation of additional models for the interaction of the undulatory mechanism with its environment, and the expansion of the developed segmental oscillators. Related resources (papers, videos, experiments, etc.) regarding applications of SIMUUN can be found at the Web site *www.ics.forth.gr/bioloch*.

Acknowledgements

This work was supported in part by the European Commission, through the Future and Emerging Technologies program (IST-FET), under grant IST-2001-34181 (project BIOLOCH).

References

[1] S. Hirose, *Biologically Inspired Robots: Snake-Like Locomotors and Manipulators*. New York: Oxford University Press, 1993.

[2] J. Ostrowski and J. Burdick, "The geometric mechanics of undulatory robotic locomotion," *International Journal for Robotics Research*, vol. 17, pp. 683–701, 1998.

[3] P. Krishnaprasad and D. Tsakiris, "Oscillations, SE(2)-snakes and motion control: A study of the roller racer," *Dynamical Systems*, vol. 16, no. 4, pp. 347–397, 2001.

[4] M. Saito, M. Fukaya, and T. Iwasaki, "Modeling, analysis, and synthesis of serpentine locomotion with a multilink robotic snake," *IEEE Control Systems Magazine*, vol. 22, no. 1, pp. 64–81, 2002.

[5] S. Ma, W. Li, and Y. Wang, "A simulator to analyze creeping locomotion of a snake-like robots," in *Proc. IEEE Conference on Robotics and Automation (ICRA'01)*, pp. 3656–3661, 2001.

[6] D. Tsakiris, A. Menciassi, M. Sfakiotakis, G. La Spina, and P. Dario, "Undulatory locomotion of polychaete annelids: mechanics, neural control and robotic prototypes," in *The Annual Computational Neuroscience Meeting*, Baltimore, USA, 2004.

[7] J. Ayers, C. Wilbur, and C. Olcott, "Lamprey robots," in *Proc. International Symposium on Aqua Biomechanisms* (T. Wu and N. Kato, eds.), 2000.

[8] K. McIsaac and J. Ostrowski, "A geometric approach to anguilliform locomotion: Modeling of an underwater eel robot," in *Proc. IEEE Conference on Robotics and Automation (ICRA'99)*, pp. 2843–3848, 1999.

[9] The MathWorks Inc., *Using Simulink - version 5.* 2003.

[10] A. Ijspeert, "A connectionist central pattern generator for the aquatic and terrestrial gaits of a simulated salamander," *Biological Cybernetics*, vol. 85, no. 5, pp. 331–348, 2001.

[11] B. Webb, "Robots in invertebrate neuroscience," *Nature*, vol. 417, pp. 359–363, May 2002.

[12] H. Olsson, K. Åström, C. de Wit, M. Gäfvert, and P. Lischinsky, "Friction models and friction compensation," *European Journal of Control*, vol. 29, no. 4, pp. 176–195, 1998.

[13] G. Taylor, "Analysis of the swimming of long and narrow animals," *Proceedings of the Royal Society (A)*, vol. 214, pp. 158–183, 1952.

[14] Ö. Ekeberg and S. Grillner, "Simulations of neuromuscular control in lamprey swimming," *Philosophical Transactions of the Royal Society of London Series B*, vol. 354, no. 1385, pp. 895–902, 1999.

[15] M. Sfakiotakis, D. Lane, and J. Davies, "Review of fish swimming modes for aquatic locomotion," *IEEE Journal of Oceanic Engineering*, vol. 24, no. 2, pp. 237–252, 1999.

[16] J. Lighthill, "Hydromechanics of aquatic animal propulsion - a survey," in *Mathematical Biofluiddynamics*, pp. 11–44, Bristol: J.W. Arrowsmith Ltd., 1975.

[17] K. D'Aout and P. Aerts, "A kinematic comparison of forward and backward swimming in the eel *Anguilla anguilla*," *Journal of Experimental Biology*, vol. 202, no. 11, pp. 1511–1521, 1999.

[18] R. Clark and D. Tritton, "Swimming mechanisms in nereidiform polychaetes," *Journal of Zoology*, vol. 161, pp. 257–271, 1970.

[19] M. Srinivasan, M. Poteser, and K. Kral, "Motion detection in insect orientation and navigation," *Vision Research*, vol. 39, pp. 2749–2766, 1999.

[20] A. Argyros, D. Tsakiris, and C. Groyer, "Biomimetic centering behavior for mobile robots with panoramic sensors," *IEEE Robotics and Automation Magazine*, vol. 11, no. 4, pp. 347–397, 2004.